JOURNAL OF MAGNETIC RESONANCE **133,** 273–280 (1998)
ARTICLE NO. MN981462

Analysis of the REDOR Signal and Inversion

Jean-Baptiste d'Espinose de la Caillerie and Christian Fretigny

Laboratoire de Physique Quantique, URA CNRS 1428, Ecole Supérieure de Physique et de Chimie Industrielles de la Ville de Paris, 10 rue Vauquelin, 75231 Paris Cedex 05, France

Received November 25, 1997; revised March 18, 1998

An inversion of the REDOR signal to recover the dipolar couplings has been recently proposed [K. T. Mueller *et al., Chem. Phys. Lett.* 242, 535 (1995)]: The corresponding integral transform was performed by tabulation of the kernel followed by numerical integration. After explicit determination of the inverse REDOR kernel by the Mellin transform method, we propose an alternative inversion method based on Fourier transforms. Representation of the inverse REDOR kernel by its asymptotic expansion reveals that the inverse REDOR operator is essentially a weighted sum of a cosine transform and of its derivative. Consequently, known properties of Fourier transforms can easily be transposed to the REDOR inversion, allowing for a precise discussion of the value of the method. Moreover, the first term of the asymptotic expansion leading to a derivative of a cosine transform, the REDOR inversion is found to be extremely sensitive to noise, thus considerably reducing the useful part of the theoretical dipolar window.

Key Words: **MAS–NMR; REDOR; inversion.**

INTRODUCTION

Because the dipolar coupling is strongly dependent on the internuclear distance, its measurement in solids by the rotational echo double resonance (REDOR) method in magic-angle spinning (MAS) solids has proven to be a valuable structural tool. Since its development by Gullion and Shaefer (*1*), numerous examples of its application in such diverse fields as biochemistry (*2–4*), inorganic chemistry (*5–7*), and catalysis (*8–11*) can be found in the literature. Basically, the REDOR experiment is a rotor-synchronized spin–echo with additional π pulses on the decoupling channel which selectively prevent refocusing of the heterodipolar dephasing. The intensity of the echo is related to the heterodipolar coupling strength and to the number of applied π pulses, while MAS averaging ensures the spectral resolution on the chemical shift axis. When π pulses are applied at half and full rotor periods during n rotor periods (Fig. 1), the heterodipolar dephasing for an isolated interacting pair has been calculated to be (*12, 13*)

$$|\Delta\phi| = 4\sqrt{2}n\frac{\nu_D}{\nu_r}\cos\alpha\sin\beta\cos\beta = 2\sqrt{2}t\nu_D\cos\alpha\sin 2\beta, \quad [1]$$

where ν_D is the heterodipolar coupling strength expressed in frequency units, ν_r is the rotor spinning frequency, t (or n/ν_r) is the evolution time, and α and β are the azimuthal and polar angles of the internuclear vector with the spinning axis. The REDOR signal normalized to the full echo is therefore given by the powder average

$$S(t\nu_D) = \frac{S}{S_0} = \frac{1}{4\pi}\int_0^{2\pi} d\alpha \int_0^{\pi} d\beta \sin\beta\cos[2\sqrt{2}t\nu_D\cos\alpha\sin 2\beta]. \quad [2]$$

For a single coupling, ν_D can be obtained by measuring the REDOR signal at one or a few values of the evolution time and by adjusting it to the theoretical expression of Eq. [2] (*2, 3, 10, 14*). For more complex distributions of couplings, or when better accuracy is desired, a full REDOR curve is recorded and adjusted (*5–7, 11*). An important limitation of this procedure is that an *a priori* knowledge of the functional form of the distribution of couplings is required.

Recently, Mueller made the seminal realization that the REDOR signal has a simple analytical form as a product of cylindrical Bessel functions of the first kind (*15*) (Appendix A)

$$S(t\nu_D) = \frac{\pi}{2\sqrt{2}}J_{1/4}(\sqrt{2}t\nu_D)J_{-1/4}(\sqrt{2}t\nu_D). \quad [3]$$

It was subsequently demonstrated that the REDOR signal could be inverted *via* a ''REDOR transform'' (*16*). This advance is particularly fertile, as it allows for the determination of the distribution of coupling without any *a priori* assumption and, consequently, permits full use of the REDOR sequence as a 2D experiment (*17*): the time evolution during the free induction decay of the echo leading to a chemical shift axis after traditional Fourier transform and the time evolution during the π pulses train leading to a purely heterodipolar axis after REDOR transform.

The object of this paper is to reveal through mathematical inspection the practical consequences of Eq. [3]. After going through the formal inversion problem, we will show that an

1090-7807/98 $25.00

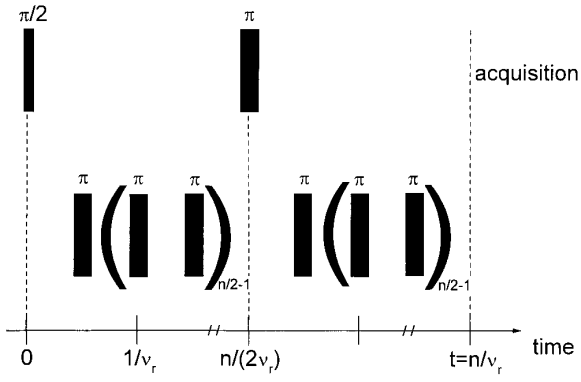

FIG. 1. A typical REDOR sequence. The number of rotor period (n) is an even number.

asymptotic expansion of the inverse REDOR kernel not only provides a convenient inversion mean, but, more importantly, gives clear insight into the potential and limits of the REDOR experiment.

THE INVERSION PROBLEM

The time domain theoretical REDOR signal defined in Eq. [3] has a decaying oscillatory form (Fig. 2). It should be noted that it is not always positive and that it decays rather sharply. Experimentally, the REDOR signal results from an unknown distribution of couplings $I(\nu_D)$

$$S_{\exp}(t) = \int_0^\infty I(\nu_D) S(t\nu_D) d\nu_D. \qquad [4]$$

If the distribution can be assumed to have a simple functional form such as the sum of a few discrete couplings or even a continuous Gaussian distribution of couplings, the integral of

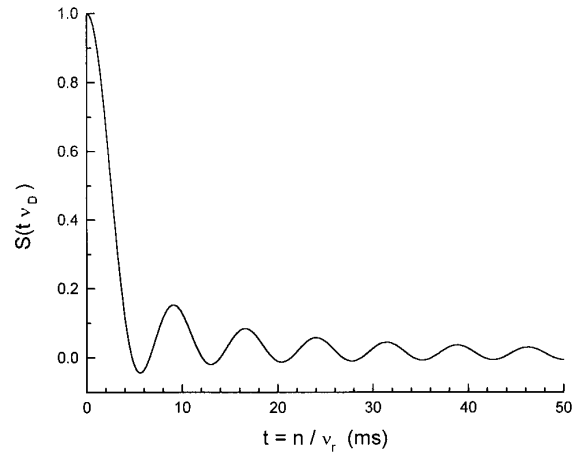

FIG. 2. Theoretical time-domain REDOR signal for an isolated pair of $\frac{1}{2}$ spins with an heterodipolar coupling of 300 Hz (Eq. [3]).

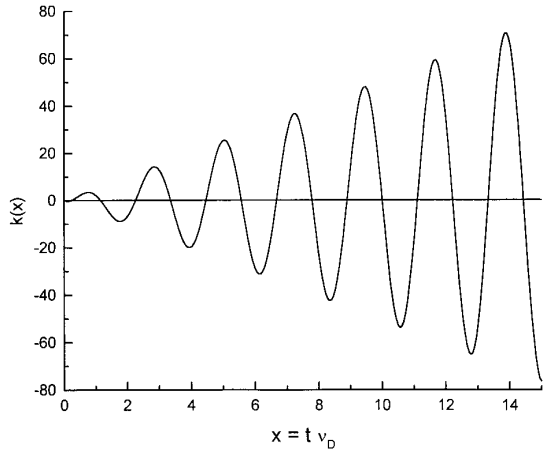

FIG. 3. The inverse REDOR kernel (Eq. [6]).

Eq. [4] can be numerically evaluated with reasonable accuracy. Alternatively, Eq. [4] can be analyzed as an integral operator acting on $I(\nu_D)$ with $S(t\nu_D)$ as a kernel. Then, recovering an unknown distribution of couplings is equivalent to finding the inverse of this operator. If a solution to this inversion problem exists in the form of an integral operator, it is possible to directly determine the frequency–domain distribution of coupling

$$I(\nu_D) = \int_0^\infty S_{\exp}(t) k(t\nu_D) dt \qquad [5]$$

provided that one is able to calculate the inverse kernel $k(t\nu_D)$. Indeed, it was first realized by Mueller that the inversion problem could be solved (*16*). $k(t\nu_D)$ can be determined using Mellin transforms (Appendix B) to be

$$k(t\nu_D) = 2\sqrt{2}t\nu_D \left\{ \begin{array}{c} J_{1/4}(\sqrt{2}t\nu_D)^2 - J_{-1/4}(\sqrt{2}t\nu_D)^2 \\ +4\sqrt{2}t\nu_D[J_{1/4}(\sqrt{2}t\nu_D)J_{-3/4}(\sqrt{2}t\nu_D) \\ + J_{-1/4}(\sqrt{2}t\nu_D)J_{3/4}(\sqrt{2}t\nu_D)] \end{array} \right\}. \qquad [6]$$

The inverse kernel has a divergent oscillatory behavior (Fig. 3) which renders the numerical evaluation (after truncation) of the integral of Eq. [5] delicate, albeit possible, because of the decaying character of $S(t\nu_D)$. Indeed, numerical evaluation of the so-called REDOR transform by a truncated sum has been shown to satisfactorily extract discrete distributions of couplings from model (*16*) as well as experimental signals (*17*).

REPRESENTATION OF THE INVERSE REDOR KERNEL

By looking at the somewhat complex expression of the inverse kernel, inversion through a numerical integration might

seem to be a computationally heavy task, necessitating evaluation of the inverse kernel and summing over the time domain at each sampled frequency. Fortunately, this is not the case. First, the temporal extension of the REDOR signal is restrained by its decaying character and the low sensitivity of NMR allowing for a limited number of significant points. Second, the kernel needs to be computed only for one frequency, as the kernel is symmetrical. There is therefore no urgent need to develop a more sophisticated inversion procedure. It is not easy though to circumscribe the potential of the REDOR inversion by looking at Eq. [6] but, as already underlined by Schaefer *et al.* (*12*, *18*), the oscillatory nature of the REDOR kernel suggests a behavior for the inverse REDOR operator similar to a Fourier transform. In this respect, an asymptotic expansion of the inverse REDOR kernel is particularly informative (*16*). A similar approach would be to expand the direct kernel, truncate it, and invert it in its approximate form. This is the route followed by McCabe and Wassall on another inversion problem, dePaking (*19*, *20*). In the present case, we expanded the exact inverse kernel, thereby gaining a more directly exploitable insight. From Hankel's asymptotic expansions of the Bessel functions of the first kind (*21*), we found

$$k(t\nu_D) = \frac{16}{\pi}\, t\nu_D \sin(2\sqrt{2}t\nu_D) - \frac{3}{\sqrt{2}\pi}\cos(2\sqrt{2}t\nu_D) - \frac{9}{64\pi}\frac{\sin(2\sqrt{2}t\nu_D)}{t\nu_D} + \frac{33\sqrt{2}}{2048\pi}\frac{\cos(2\sqrt{2}t\nu_D)}{(t\nu_D)^2} + \frac{315}{65536\ 2\pi}\frac{\sin(2\sqrt{2}t\nu_D)}{(t\nu_D)^3} + O\left(\frac{1}{(t\nu_D)^4}\right). \quad [7]$$

Replacement of the inverse REDOR kernel in Eq. [5] by this asymptotic expansion reveals that the inverse REDOR operator is essentially a weighted sum of a derivative of a cosine transform, a cosine transform, and primitives of cosine transforms. This suggests that representing the inverse REDOR kernel by its truncated asymptotic development can provide valuable insights into the behavior of the signal upon inversion.

As a preliminary, the validity of this representation can be discussed through graphical comparison of the exact kernel to the truncated asymptotic expansion (Fig. 4). The dominant term is by far the first one; however, the ratio of the first two prefactors being

$$\frac{-3}{16\sqrt{2}}\frac{1}{t\nu_D} \cong -0.13\,\frac{1}{t\nu_D},$$

the second term is expected to be significant, especially at low values of $t\nu_D$. As seen in Fig. 4, adding the second term considerably diminishes the error. The subsequent terms (the primitives of cosine or sine transforms) improve the overall representation but introduce a violent divergence at the origin

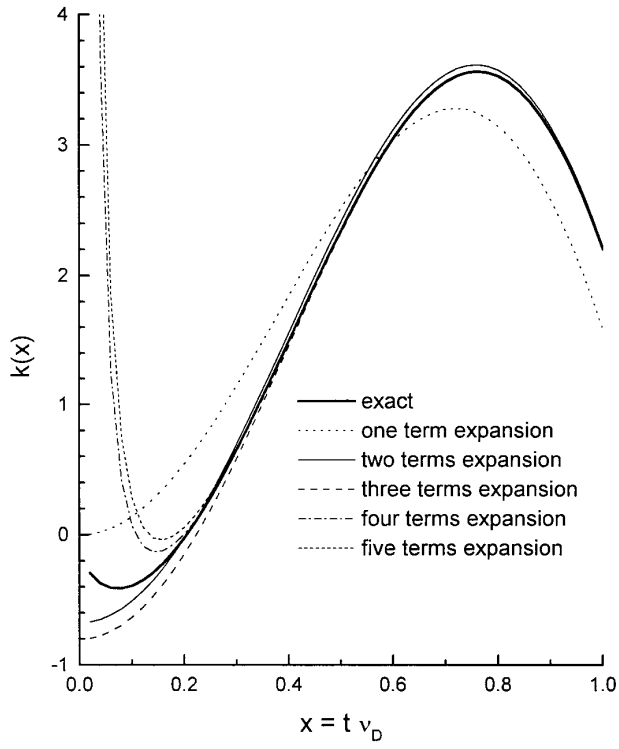

FIG. 4. The exact inverse REDOR kernel (fat solid line) and its representation by truncated asymptotic expansions.

because of the inverse powers of $t\nu_D$. The question thus arises of how many terms of the asymptotic series should be retained for an optimal representation of the kernel. At a finite value of $t\nu_D$, the first neglected term provides a good estimate of the error. Adding more and more terms, this error initially decreases but because of the divergence it is eventually going to increase after a certain number of terms (N). Truncating the series at ($N - 1$) thus provides the approximation with the smallest possible error at fixed $t\nu_D$ (*22*). Inversely, we can decide to keep only the first two terms and look for the value of $t\nu_D$ up to which the approximation is optimal. Computing the values of the individual terms of the series shows that up to $t\nu_D = 0.22$, the first two terms provide the most accurate representation, while adding more terms improves the representation for higher values of $t\nu_D$. This could be intuited by looking at the graphical representation of the kernel and of the series truncated at different orders in Fig. 4. In conclusion, truncation after the second term is preferable at low frequency but adding more terms will, in theory, provide a better representation of higher frequencies. At intermediate frequencies the best theoretical representations would require a composite truncation: two terms below $t\nu_D = 0.22$ and additional terms beyond that value.

At this point it is useful to consider the experimental implication of this cutoff value of $t\nu_D$. As an illustration of this, truncation after the second term provides the least error only up to about 5 Hz for a typical temporal extension of 50 ms. On the

other hand, with typical spinning at 10 kHz, the first sampling point is at 0.2 ms, which means that adding more than two terms would improve the representation for frequencies higher than about 1 kHz. Theoretically, a composite representation is thus optimal for frequencies between 5 Hz and 1 kHz in this case. This, however, somewhat complicates the matters, and we prefer to represent the kernel across the frequency range with a single analytical form, that is, as its asymptotic expansion truncated after the second term. If, as we will show, this representation is satisfactory, the REDOR inversion simply amounts to a weighted sum of a cosine transform and of its derivative,

$$I(\nu_D) \cong -4\nu_D \frac{\partial}{\partial \nu_D} \mathcal{C}[(S(t'))] - \frac{3}{2} \mathcal{C}[(S(t'))], \qquad [8]$$

where $\mathcal{C}$ stands for the cosine transform operator and where the change of variable $t' = (\sqrt{2}/\pi)t$ accounts for the definition of the kernel of the Fourier transform as $e^{-i2\pi t' \nu_D}$.

In order to further test and illustrate the validity and significance of this representation, we have constructed a typical test signal composed of four isolated pair contributions (Fig. 5). Comparison of the exact signal inverted by numerical integration using a tabulated kernel (Eq. [5]) with the approximate one inverted *via* Fourier transforms (Eq. [8]) indeed validates our approach. Upon inversion, adding the second term (the cosine transform) to the first one (the derivative of the cosine transform) leads to a significant baseline correction. Theoretically, as shown above, the baseline could be further improved for low frequencies (below 1 kHz in the example presented in Fig. 5) by adding more terms. Practically however, it is apparent through comparison with the exact inverted signal in Fig. 5 that truncating after the second term results only in a small baseline error across the whole frequency range. Furthermore, as will be shown below, the effect of experimental noise on the first term far exceeds the correction due to the subsequent terms. Overall, the representation of the kernel by its asymptotic series truncated after the second term is therefore entirely satisfactory.

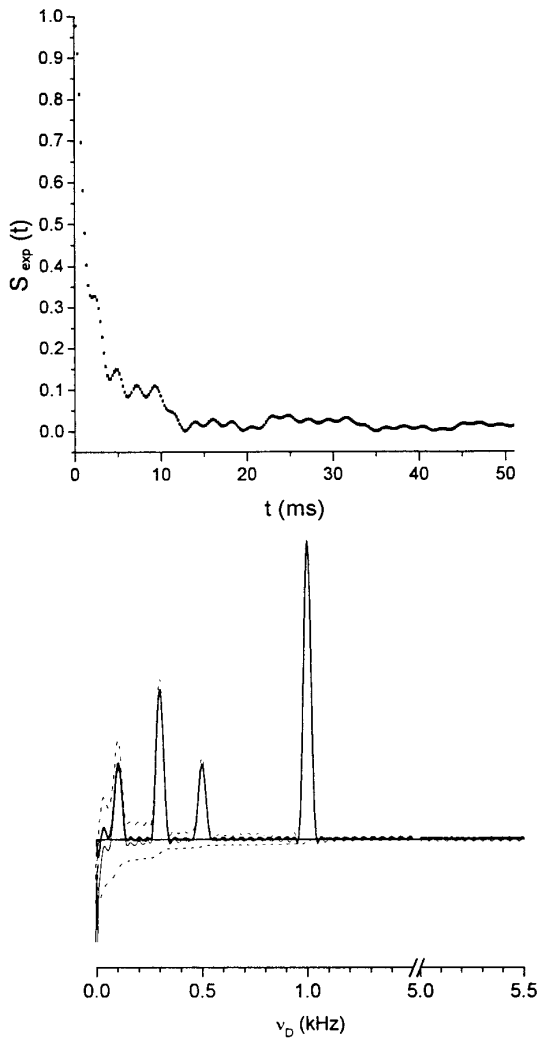

FIG. 5. Inversion (bottom) of a simulated signal (top) of 256 points (temporal extension of 51 ms) obtained at $\nu_r = 10$ kHz consisting of four discrete pairs of couplings of frequencies and relative intensities: $\frac{1}{8}$ at 100 Hz, $\frac{1}{4}$ at 300 Hz, $\frac{1}{8}$ at 500 Hz, and $\frac{1}{2}$ at 1 kHz. Zero filling to 2048 points, apodization by a Kaiser ($\tau = 5$) window (Ref. (*23*)). Dotted lines: contributions of the first (positive) and second (negative) term of the expansion. Solid line: sum of the first two contributions of the expansion (Eq. [8]). Thick line: inversion by numerical integration.

DISCUSSION

Whatever the order at which the asymptotic series is truncated, the representation of the kernel by its asymptotic expansion has real advantages. First, it provides computational stability. Replacing the inverse REDOR operator of Eq. [5] by a sum of Fourier transforms (Eq. [8]), instead of by a numerical integration as has been performed by previous authors (*16, 17*), provides a more robust inversion procedure. Indeed, algorithms for Fourier transforms are easily available, fast, and stable. One must nevertheless recognize that the computational advantage of the asymptotic expansion representation is minimal and that choosing to execute Fourier transform algorithms rather than to tabulate the exact kernel is more a matter of taste and esthetics than a true necessity.

Perhaps more importantly, the asymptotic expansion helps to prepare and understand the REDOR experiment. It reveals that the inverse REDOR operator shares properties with Fourier transforms. Indeed, the asymptotic expansion provides firm grounds to transpose, from Fourier transforms to REDOR transforms, the relationships between the time domain and the frequency domain well known to NMR spectroscopists.

We will explore the significance of this finding by observing the effects of experimental constraints such as the limitation of the temporal window, discrete sampling, and noise on the inverted dipolar spectrum of a model signal. These effects,

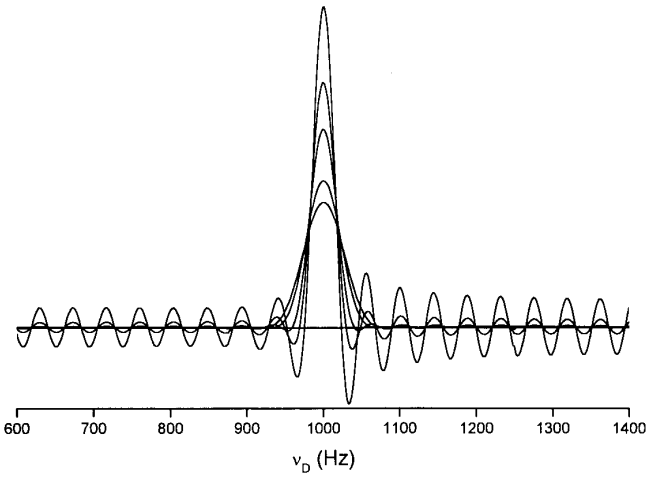

FIG. 6. Effect of a Kaiser window of increasing width (Ref. (*23*)) $\tau = 1$, 3, 5, 10, 100 on the simulated REDOR signal of a single pair ($\nu_D = 1$ kHz). Other characteristics of the simulation are as in Fig. 5.

which are not obvious by inspecting Eq. [6], are easily predicted from Eq. [8]. For example, zero filling in the time domain results in interpolation in the frequency domain. Also, Eq. [8] helps predict the behavior of the line shape regarding truncation and apodization (Fig. 6). The effect of the Kaiser window (*23*) is tested on a model signal.[1] The usual line width *versus* ripple behavior of Fourier transforms is indeed observed here. But maybe the more useful insight is provided by the relationship between the temporal extension of the signal and the resolution (and cutoff) in the dipolar frequency domain. This point is illustrated by comparison of the idealized inverted REDOR signal of Fig. 5 with the more realistic simulation of Fig. 7, where the temporal extension has been limited. Experimental shortening of the temporal extension of the REDOR signal leads to a significant loss of resolution. Representation by Fourier transforms allows use of the Nyquist theorem, leading to a formal expression for the resolution

$$\Delta\nu_D = \nu_{D_{\min}} = \frac{\pi\nu_r}{2\sqrt{2}n_{\max}} = \frac{\pi}{2\sqrt{2}t_{\max}} \qquad [9]$$

as well as for the dipolar frequency spectral width

$$\nu_{D_{\max}} = \frac{\pi}{2\sqrt{2}\Delta t} = \frac{\pi\nu_r}{4\sqrt{2}}. \qquad [10]$$

Note also in Fig. 6 how the width of the lines is dominated by the width of the window τ (a necessity to avoid excessive ripples) rather than by the temporal extension.

A limitation of practical importance of the REDOR transform can be easily comprehended from Eqs. [9] and [10]. Probing nontrivial multiple bonds connectivity requires measurements of couplings of less than 40 Hz. Direct numerical application shows that while the dipolar window defined by Eq. [10] is largely sufficient, Eq. [9] leads to experimentally unrealistic evolution times (larger than 28 ms).

A less trivial question can also be successfully discussed by representing the inverse REDOR kernel by its asymptotic expansion; that is, what is the stability with regard to noise? We have performed the inversion of a simulated signal containing a normal distribution of noise of 2% variance (Fig. 8). Despite this relatively low noise level, the inverted REDOR spectrum exhibits ample oscillations. The dominant term of the asymptotic expansion of the inverse kernel is the derivative cosine transform which means that the noise is scaled by $t\nu_D$. This introduces a rather violent divergence which is much more taxing that what can be encountered in the usual NMR

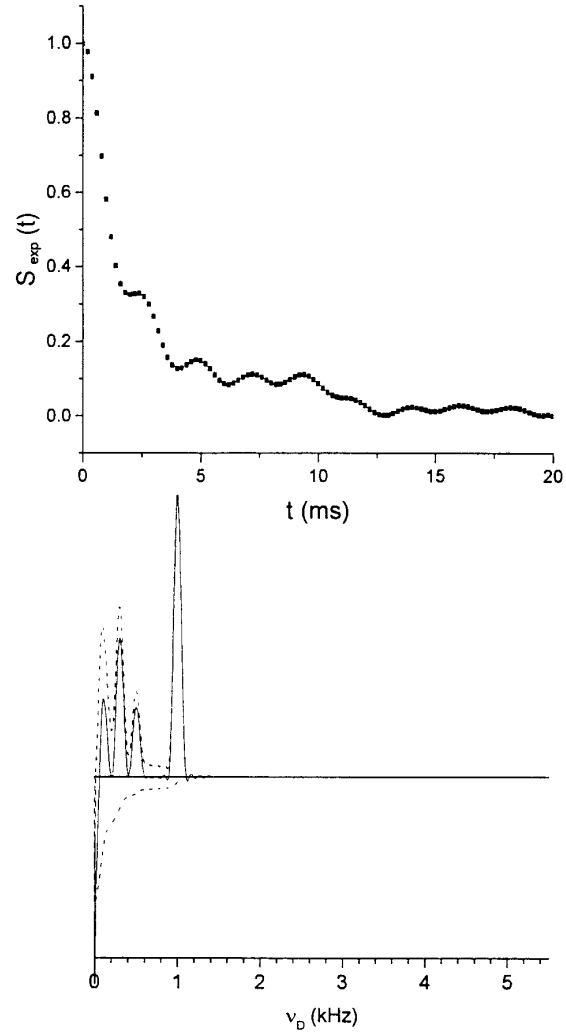

FIG. 7. Inversion (bottom) of a simulated signal (top) of 50 points obtained at $\nu_r = 10$ kHz of the same characteristics as in Fig. 5. Zero filling to 2048 points, apodization by a Kaiser ($\tau = 5$) window. Inversion by cosine transforms (Eq. [8]).

[1] This window involving a modified zero-order Besel function I_0 has the main advantage of providing an adjustable width parameter τ through $h(t) = I_0(\tau\sqrt{1 - 4(t/t_{\max})^2})/I_0(\tau)$.

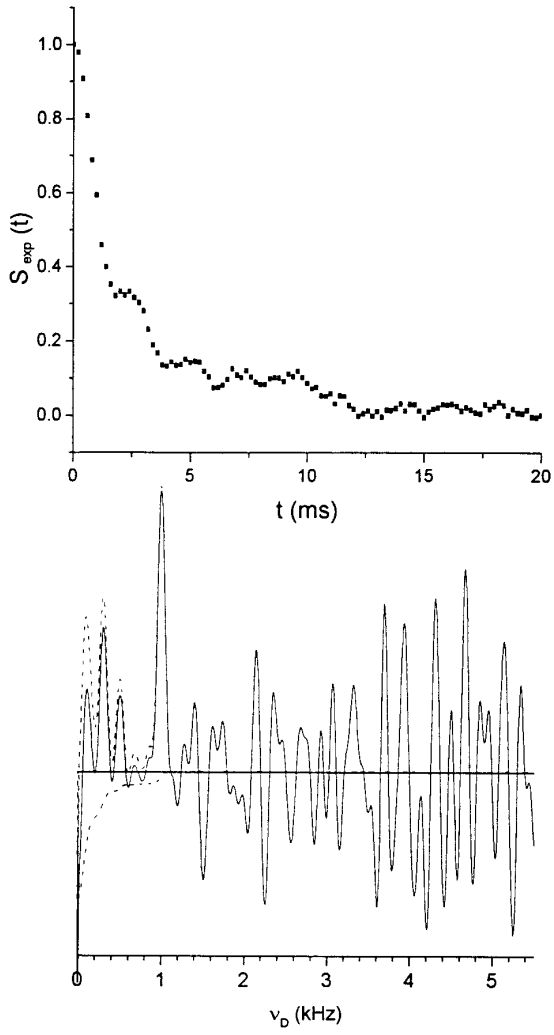

FIG. 8. Inversion (bottom) of a simulated signal (top) of 50 points obtained at $\nu_r = 10$ kHz of the same characteristics as in Fig. 5 with noise of normal distribution and 2% variance. Zero filling to 2048 points, apodization by a Kaiser ($\tau = 5$) window. Inversion by cosine transforms (Eq. [8]).

inversion problems, or even in dePaking (*20*), where the signal is an FID. Indeed, the rapid exponential decay of an FID allows for a faster divergence of the relevant kernel than the $1/t\nu_D$ decay of the REDOR signal of Eq. [3]. Scaling of the noise by $t\nu_D$ has two direct implications. First, the noise will not be homogeneously distributed across the spectral window, but its variance will be amplified with increasing frequency ν_D, in effect reducing the theoretical dipolar window defined by Eqs. [9] and [10] to a maximum practical value of 1.5 kHz in this example. Second, noise occurring at a later time will have a more pronounced impact than that occurring at an earlier time and will significantly deteriorate the resolution which is linked to the quality of the signal at long time through Eq. [9]. This last point is particularly irritating, as the level of noise is precisely expected to be higher in the REDOR experiment at longer times. Indeed, the REDOR signal is scaled relatively to the full echo signal S_0. As time increases, the echo signal decreases due to transverse relaxation, resulting in a deterioration of the signal to noise ratio. Moreover, since the sampling time is determined by the number of π pulses applied, errors in the pulse's phase, amplitude, and synchronization with the rotor period accumulate at long time, again resulting in a larger deviation from the theoretical form of the REDOR curve.

Theoretically, the deterioration of the REDOR effect at long time is not solely due to experimental inaccuracies that could be minimized by careful setting and phase cycling. Indeed, the relevance of the REDOR equation (Eq. [1]) is limited to isolated spin pairs, and such a hypothesis is unlikely to hold strictly at long time when the contribution of distant spins becomes significant. The significance of the contribution of the distant spins to the broadening of the signal can be discussed within the framework of the REDOR transform. As a typical example, one can consider a REDOR signal with a temporal extension of 20 ms and resulting from a dipolar coupling of 500 Hz. Equation [9] then leads to a limit experimental width of 56 Hz (never attained because of the necessary application of a windowing function). REDOR signals resulting from multiple spin heteronuclear couplings, that is a $I - S_n$ system rather than the single pair $I - S$, have been analyzed by previous authors in the time domain, neglecting the effect of the homonuclear coupling (*2, 24*), and it is well established that contributions from several spins result in a heterogeneous distribution of couplings (*25*). For instance the $I - S_2$ linear system leads to two dipolar frequencies at the sum and difference of the two individual pairs. In the present case, given that ν_D evolves as r^{-3}, this means that the limit experimental width of 56 Hz would deteriorate due to interaction with the second I spin only if it were less than twice as remote—an unlikely event for a regular array of rare spins. The effect of the distant spin on the signal is therefore unobservable in most cases (for rare spins), and the treatment in terms of isolated spin pair (and thus everything we derived from Eq. [3]) is *a posteriori* justified. This discussion exemplifies the kind of simple and useful insights provided by the REDOR transform.

SUMMARY

Mathematical inspection of the REDOR inversion proposed by Mueller allowed us to better understand the quality of the information provided by the REDOR experiment. Representation of the inverse REDOR kernel by its asymptotic expansion revealed experimentally relevant properties of the inverse REDOR operator. The latter was found analogous to a weighted sum of a cosine transform and of its derivative. Besides providing a new alternative inversion procedure, this finding formalized intuitive relationships between the temporal signal and its dipolar transform. Noticeably, it was found that the spectral width and resolution in the dipolar dimension are mainly limited by the instability of the inversion procedure with regard to noise. Beyond its immediate relevance to the REDOR in-

version, the type of mathematical preparation performed in this work might prove useful in other MAS–NMR experiments exhibiting oscillatory, nonperiodic signals for which a straightforward Fourier analysis is not necessarily the most efficient method.

APPENDIX A

Direct Determination of the Analytical Form of the REDOR Signal

The REDOR signal normalized to the full echo signal is given by the powder average

$$\frac{S}{S_0} = \frac{1}{4\pi}\int_0^{2\pi} d\alpha \int_0^{\pi} d\beta \sin\beta \cos[2\sqrt{2}t\nu_D \cos\alpha \sin 2\beta].$$

As recognized by Mueller, solution of such an integral of trigonometric functions of trigonometric functions will obviously involve Bessel functions. However, the expansion of the trigonometric functions into an infinite sum of Bessel function (*15*) followed by identification of the infinite sum with a product of Bessel functions (*16*) is an unnecessary step. Integrating over α, one gets (*26*)

$$\frac{S}{S_0} = \frac{1}{2}\int_0^{\pi} d\beta \sin\beta J_0(2\sqrt{2}t\nu_D \sin 2\beta),$$

which directly leads after integration over β to (*27*)

$$S(t\nu_D) = \frac{\pi}{2\sqrt{2}} J_{1/4}(\sqrt{2}t\nu_D) J_{-1/4}(\sqrt{2}t\nu_D).$$

APPENDIX B

Determination of the REDOR Kernel Using Mellin Transforms

Generality: Determination of an Inverse Kernel Using Mellin Transforms

Given an integral operator which kernel h is a function of the product of the variable x and of the integration variable y,

$$F(x) = \int_0^{\infty} f(y)h(xy)dy, \qquad [B.1]$$

the Mellin transformation allows determination of the inverse integral operator $f(y)$ if it exists (*28*):

$$f(y) = \int_0^{\infty} F(y)k(xy)dx. \qquad [B.2]$$

Both kernels are related through the relation

$$H(s)K(1-s) = 1, \qquad [B.3]$$

where $H(s)$ and $K(s)$ are the Mellin transforms of h and k. Obviously, this relation must be verified in a region of s such that the functions $H(s)$ and $K(s)$ must be defined on s and $(1 - s)$. The Mellin transform and its inverse are

$$H(s) = \int_0^{\infty} u^{s-1}h(u)du \qquad [B.4]$$

and

$$h(u) = \frac{1}{2i\pi}\int_{c-i\infty}^{c+i\infty} u^{-s}H(s)ds, \qquad [B.5]$$

where c is real and must belong to the absolute convergence band of H, that is the interval into which $\Re(s)$ satisfies the convergence of H.

Finally, Eqs. [B.3] and [B.4] lead to the expression of the inverse kernel,

$$k(u) = \frac{1}{2i\pi}\int_{c-i\infty}^{c+i\infty} \frac{u^{-s}}{H(1-s)}ds, \qquad [B.6]$$

where again c must be such that $H(s)$ and $H(1 - s)$ are analytical.

Application to the REDOR Inversion

The aim is to recover the unknown distribution of coupling from the experimental signal. Identifying the experimental signal of Eq. [4] with the integral operator of Eq. [B.1] and the REDOR signal of Eq. [3] with the direct kernel, one can define the inverse REDOR kernel $k(t\nu_D)$ and the inverse REDOR operator as

$$I(\nu_D) = \int_0^{\infty} S_{\exp}(t)k(t\nu_D)dt. \qquad [B.7]$$

Determination of the Inverse REDOR Kernel

In an article from 1969 (*29*), a kernel defined as the product of two cylindrical Bessel functions of orders differing by an integer was inverted using the Mellin transform method. Although the orders of the Bessel functions involved here (Eq.

[3]) differ by a half-integer, the formula derived in (*29*) was used by Mueller to perform the REDOR inversion (*16*), and the deviation from the true inverse REDOR kernel was deemed minimal (*30*). Nevertheless, the true inverse REDOR kernel can be obtained by the same Mellin transform method followed in Ref. (*29*). The Mellin transform (Eq. [B.4]) of the direct kernel of Eq. [3] is (*31*)

$$H(s) = 2^{1-s}\frac{\Gamma(1-s)\Gamma(s/2)}{\Gamma(5/4-s/2)\Gamma(1-s/2)\Gamma(3/4-s/2)}$$
$$0 < \Re(s) < 1, \qquad \text{[B.8]}$$

leading, from Eq. [B.5], to the expression of the inverse REDOR kernel

$$k(u) = \frac{1}{2i\pi}\int_{c-i\infty}^{c+i\infty}(u)^{-s}2^{s} \times \frac{\Gamma(1/4+s/2)\Gamma(1/2+s/2)\Gamma(3/4+s/2)}{\Gamma(1/2-s/2)\Gamma(s)}\,ds. \qquad \text{[B.9]}$$

This integral is evaluated using the residue theorem. The result, expressed as a series, is transformed as in Ref. (*29*) and leads to

$$k(u) = 4\pi\sqrt{2}u\frac{d}{du}\{u[J_{1/4}(u)^2 - J_{-1/4}(u)^2]\}, \qquad \text{[B.10]}$$

which can be expressed in the more useful form

$$k(u) = 2\pi\sqrt{2}u\{J_{1/4}(u)^2 - J_{-1/4}(u)^2 + 4u[J_{1/4}(u)J_{-3/4}(u) + J_{-1/4}(u)J_{3/4}(u)]\}.$$

Finally, after making the necessary change of variables to account for the fact that the argument of the Bessel functions is $(\sqrt{2}t\nu_D)$ where the coupling ν_D is expressed in frequency units, one gets the formula given in the text (Eq. [6]).

ACKNOWLEDGMENTS

The assistance of two students of the ESPCI, Anna Rakovska and Arnaud Pecquet, proved to be very valuable for the realization of this project.

REFERENCES

1. T. Gullion and J. Schaefer, *J. Magn. Reson.* **81,** 196 (1989).
2. L. M. McDowell, D. Barkan, G. E. Wilson, and J. Schaefer, *Solid State Nucl. Magn. Reson.* **7,** 203 (1996).
3. A. Naito, K. Nishimura, S. Kimura, S. Tuzi, M. Aida, N. Yasuoka, and H. Saitô, *J. Phys. Chem.* **100,** 14995 (1996).
4. Y. Li, J. Appleyard, W. A. Shuttleworth, and J. N. S. Evans, *J. Am. Chem. Soc.* **116,** 10799 (1994).
5. Y. Pan, *Solid State Nucl. Magn. Reson.* **5,** 263 (1995).
6. S. M. Holl, T. Kowalewski, and J. Schaefer, *Solid State Nucl. Magn. Reson.* **6,** 39 (1996).
7. C. Hudalla, H. Eckert, and R. Dupree, *J. Phys. Chem.* **100,** 15986 (1996).
8. A. L. Blumenfeld, D. Coster, and J. J. Fripiat, *J. Phys. Chem.* **99,** 15181 (1995).
9. A. L. Blumenfeld, D. J. Coster, and J. J. Fripiat, *Chem. Phys. Lett.* **231,** 491 (1994).
10. E. R. H. van Eck, A. P. M. Kentgens, H. Kraus, and R. Prins, *J. Phys. Chem.* **99,** 16080 (1995).
11. C. P. Grey and B. S. A. Kumar, *J. Am. Chem. Soc.* **117,** 9071 (1995).
12. T. Gullion and J. Schaefer, *J. Adv. Magn. Reson.* **13,** 57 (1989).
13. Y. Li and J. N. S. Evans, *J. Chem. Phys.* **101,** 10211 (1994).
14. Y. Li and J. N. S. Evans, *J. Magn. Reson. A* **109,** 256 (1994).
15. K. T. Mueller, *J. Magn. Reson. A* **113,** 81 (1995).
16. K. T. Mueller, T. P. Jarvie, D. J. Aurentz, and B. W. Roberts, *Chem. Phys. Lett.* **242,** 535 (1995).
17. T. P. Jarvie, G. T. Went, and K. T. Mueller, *J. Am. Chem. Soc.* **118,** 5330 (1996).
18. A. Schmidt, R. A. McKay, and J. Schaefer, *J. Magn. Reson. A* **96,** 644 (1992).
19. M. A. McCabe and S. R. Wassall, *J. Magn. Reson. B* **106,** 80 (1995).
20. M. A. McCabe and S. R. Wassall, *Solid State Nucl. Magn. Reson.* **10,** 53 (1997).
21. M. Abramowitz and I. A. Stegun, ''Handbook of Mathematical Functions,'' p. 364, 9.2.5, Dover, New York (1965).
22. C. M. Brender and S. A. Orszag, ''Advanced Mathematical Methods for Scientists and Engineers,'' p. 94, International Series in Pure and Applied Mathematics, McGraw–Hill, New York (1978).
23. R. R. Ernst, G. Bodenhausen, and A. Wokaun, ''Principles of Nuclear Magnetic Resonance in One and Two Dimensions,'' p. 103, Clarendon Press, Oxford (1987).
24. A. Naito, K. Nishimura, S. Tuzi, and H. Saitô, *Chem. Phys. Lett.* **229,** 506 (1994).
25. J. H. Van Vleck, *Phys. Rev.* **74,** 1168 (1948).
26. M. Abramowitz and I. A. Stegun, ''Handbook of Mathematical Functions,'' p. 360, 9.1.18, Dover, New York (1965).
27. I. S. Gradshteyn and I. M. Ryzhik, *in* ''Tables of Integrals, Series and Products'' (A. Jeffrey, Ed.), 5th ed., p. 756, 6.681.8, Academic Press, San Diego (1994).
28. S. Columbo, ''Les Transformations de Mellin et de Hankel,'' CNRS, Paris (1959). I. N. Sneddon, ''Fourier Transforms,'' International Series in Pure and Applied Mathematics, McGraw–Hill, New York (1951).
29. W. Sollfrey, *J. Math. Phys.* **10,** 1429 (1969).
30. K. T. Mueller, T. P. Jarvie, D. J. Aurentz, and B. W. Roberts, *Chem. Phys. Lett.* **254,** 281 (1996).
31. I. S. Gradshteyn and I. M. Ryzhik, *in* ''Tables of Integrals, Series and Products'' (A. Jeffrey, Ed.), 5th ed., p. 715, 6.574.2, Academic Press, San Diego (1994). [Beware of an error in earlier editions.]